Fabrication of high-*Q* chalcogenide photonic crystal resonators by e-beam lithography

Yinlan Ruan[a)]
Center of Expertise in Photonics, School of Chemistry and Physics, University of Adelaide, Adelaide 5005, Australia

Myung-Ki Kim and Yong-Hee Lee
Nanolaser Laboratory, Department of Physics, Korea Advanced Institute of Science and Technology, Daejeon 305-701, Korea

Barry Luther-Davies and Andrei Rode
Center for Ultra-High Bandwidth Devices for Optical Systems, Laser Physics Center, The Australian National University, Canberra 0200, Australia

(Received 9 October 2006; accepted 13 January 2007; published online 12 February 2007)

The authors report design, fabrication, and characterization of photonic crystal nanocavities in nonlinear chalcogenide glass using e-beam lithography and chemically assisted ion beam etching. The design indicated that three-hole missing cavities with simultaneously modified side hole position and radii showed the maximum quality factor of 14 000, which was insensitive to the fabrication error of side holes. The fabricated cavities presented coupling dips of −2.6 dB at the wavelength of 1550 nm and quality factors up to 10 000 when excited with the evanescent field from a tapered optical fiber. © *2007 American Institute of Physics*. [DOI: 10.1063/1.2476416]

Optical bistability in a photonic crystal (PC) resonator can be used for all-optical processes such as optical logic and all-optical modulation and switching. These devices use the characteristic nonlinearity of the host material combined with ultrasmall mode volume in the resonator to obtain low operating power. Silicon is the most common material used for PC fabrication because of its high refractive index.[1,2] The observed nonlinearities in Si PC resonators have been mainly attributed to thermo-optical or free carrier effects arising from two-photon absorption (TPA). Low switching power could be obtained using high quality (Q) factor resonators.[2] The thermo-optic nonlinear response, however, limits the switching speed to a few hundred nanoseconds.[1] In order to obtain faster switching speeds while maintaining the low switching power, materials with high Kerr nonlinearity and low TPA at the telecommunication wavelengths are desirable.

Chalcogenide glasses are generally found to have Kerr nonlinearity of (100–1000) times silica and compositions with much higher nonlinearity have been reported.[3] The large nonlinearity and high refractive index (2.3–3 at 1.55 μm) have already allowed small mode area planar waveguides to demonstrate sufficiently strong self-phase modulation for all-optical regeneration.[4,5] The high refractive index of the chalcogenides also makes them attractive for PC fabrication allowing mode volume to be reduced to obtain low operating power. To date two-dimensional (2D) PC devices have been fabricated using focused ion beam milling[6] and strong coupling into PC defect mode waveguides has been demonstrated using the fiber coupling technique.[7]

In this letter, we report the design and fabrication of suspended chalcogenide PCs and nanocavities using e-beam lithography and chemically assisted ion beam etching (CAIBE). Our measurements show that these cavities displayed strong resonance with Q factors up to 10 000, which should be sufficient for low power fast all-optical bistable switching.

Films of AMTIR-1 ($Ge_{33}As_{12}Se_{55}$) glass whose Kerr nonlinearity is ≈250 times silica were deposited onto oxidized silicon wafers at room temperature using pulsed laser deposition. The measured index of the resulting films was found to be 2.7 at 1.55 μm. The basic PC design consisted of a triangular lattice of air holes in an air-clad 2D 300 nm thick PC slab. The lattice constant a was 550–600 nm and the radius of holes was fixed at $r=0.3a$. In this case, a TE-like band gap exists in the range of $(0.35–0.4)2\pi c/a$. For this demonstration of chalcogenide PC resonators, we employed three-hole missing ($L3$) cavity structures with side hole shift and/or radius reduction. Their resonant mode profiles and predicted Q factors were obtained using the three-dimensional finite difference time domain (FDTD) method.

For the cavities where only the side hole was shifted, our calculations showed that the Q factors first increased drastically and then decreased with increasing shift, in agreement with Ref. 8. A maximum Q factor of 8000 was obtained at the displacement $\Delta L=0.17a–0.21a$. For the cavities with combination of side hole shift and reduced radius, we calculated Q factors by scanning r for different side hole positions to obtain the data shown in Fig. 1. It can be seen that without the side hole shift the cavity Q factors increase sharply to a peak before decreasing slightly with a further reduction in radius. When a displacement is introduced, the Q factors show a similar trend but become insensitive to the hole radius around $r\approx0.125a$. The highest Q factor of 14 000 was obtained for $\Delta L=0.17a–0.21a$ with side hole radius $r=0.1–0.16a$. The maximum obtainable Q factor is reduced when $\Delta L>0.22a$, and the optimum radius shifts towards larger values. From experience with our particular e-beam lithography system, we have found it more difficult to accurately control hole radius than position due to instability in beam current. In addition, small holes generally have higher surface roughness compared with large holes for the same

[a)]Electronic mail: yinlan.ruan@adelaide.edu.au

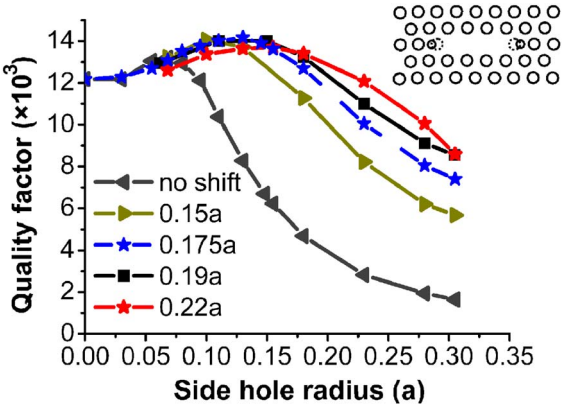

FIG. 1. (Color online) Calculated Q factors for the cavities with both side hole shifts and reduced radius.

process conditions. Therefore, we fabricated structures most tolerant to fabrication errors that corresponded to the use of larger shifts and larger holes.

The PC structures were written into a 160 nm thick polymethyl methacrylate (PMMA) photoresist layer using a converted Hitachi S4300 scanning electron microscopy (SEM) system. After development, the samples were hardened using Ar gas. CAIBE using a Cl_2/Ar gas mixture at 120 °C was used to transfer the PMMA mask pattern into the AMTIR-1 layer. Etching was carried out at a beam voltage of 600 V and 0.8 mTorr pressure with a Cl_2 flow of 2 SCCM (SCCM denotes cubic centimeter per minute at STP) and Ar flow of 3.5 SCCM. The etch rate of the AMTIR-1 was 210 nm/min. A relatively low PMMA selectivity of 1.8 over AMTIR-1 was observed due to the softness of the PMMA. We tried to improve the selectivity by increasing the substrate temperature to 200 °C without success.

As a result high-dose e-beam irradiation was tried as a means of prehardening the PMMA. In normal e-beam lithography, molecular chains in PMMA undergo scission and this makes the PMMA soluble in some developers. However, the mechanical properties such as hardness of the polymer can be dramatically improved by high-dose electron irradiation as a result of cross-linking.[9] It was found that PMMA surfaces exposed with high electron doses were darker than those exposed at low dose or without e-beam irradiation due to the formation of hydrogenated amorphous carbon.[9] From Figs. 2(a) and 2(b), we compare the surface quality of the PC samples without irradiation with those exposed at a dose of 1.35 C/cm^2. Both samples were etched at the same time and their surface is covered by the residual PMMA. As can be seen, the PMMA surface in Fig. 2(a) was rough due to overetching, while for the irradiated sample the surface was smooth and the structures were more uniform because of the improved PMMA hardness and etch selectivity. To etch through the 300 nm AMTIR-1 layer, the electron dose for PMMA prehardening needs to be greater than 2 C/cm^2. After CAIBE, the PMMA layer was removed by O_2 ashing.

It was found that the sidewalls of the etched holes were slightly slanted. Since nonvertical sidewalls can cause additional propagation loss and reduced Q factors due to coupling of TE-like mode to TM-like mode,[10] process optimization to obtain vertical sidewalls is important. In this context, the effect of the Cl_2 gas flow on sidewall angle was studied while the other parameters of the CAIBE were kept constant (the pressure depended on the Cl_2 flow). The results are

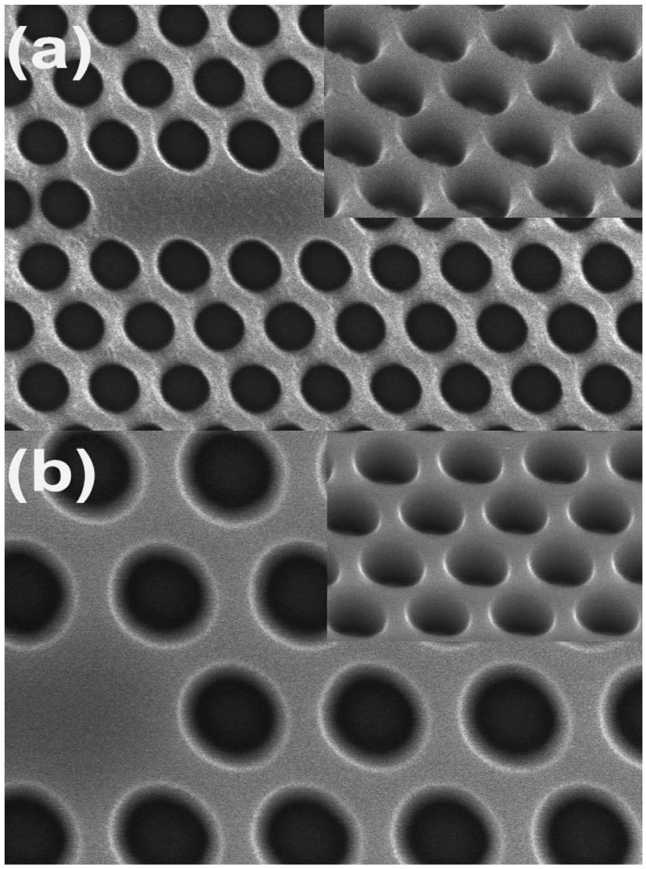

FIG. 2. (a) Etch pattern without irradiation; (b) etch patterns exposed at a dose of 1.35 C/cm^2. The insets are corresponding SEM images at 45° tilt.

shown in Fig. 3. The inserted SEM image is the cross-sectional profile for a sample etched at a Cl_2 flow rate of 9.5 SCCM. Figure 3 shows that the sidewall became more vertical at higher flow rates and near vertical sidewalls (angle 88.6°) could be obtained when the Cl_2 gas flow rate was increased to 12 SCCM.

To obtain air-clad suspended PCs, the oxidized silicon layer underneath the AMTIR-1 layer was finally etched away by using buffered oxide etching. A series of cavity samples was fabricated by using the optimized processes. Their resonant modes were characterized using the evanescent fiber taper coupling as described in Ref. 11.

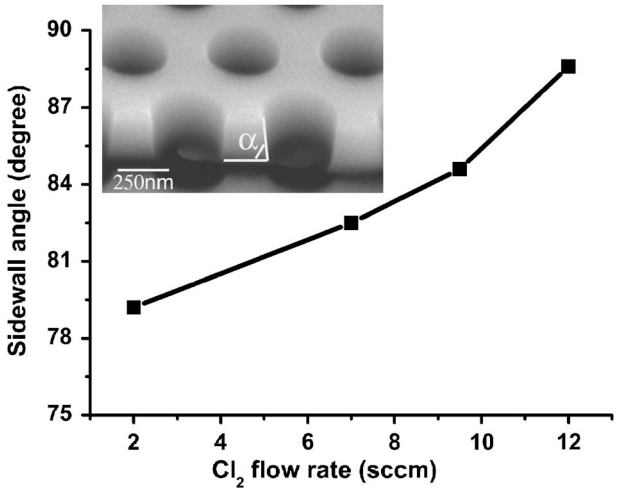

FIG. 3. Sidewall angle dependence on Cl_2 flow rate during CAIBE.

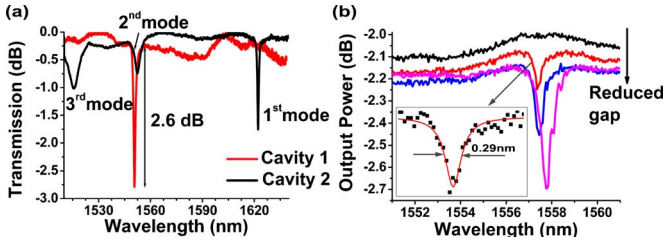

FIG. 4. (Color online) (a) Transmission spectra for cavity 1 with $\Delta L=0.2a$ and $r=0.21a$ and cavity 2 with $\Delta L=0.15a$. (b) Dependence of transmission on fiber-cavity separation.

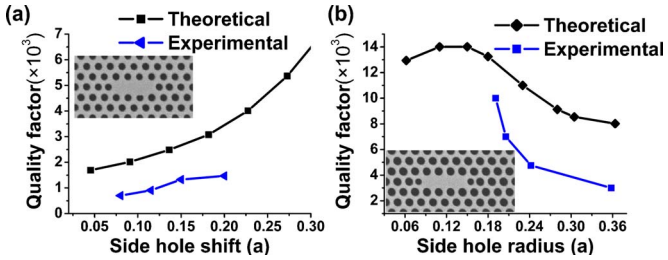

FIG. 5. (Color online) Comparison of the experimental Q factors with numerical predictions for cavities with (a) side hole shift alone, and (b) $\Delta L=0.2a$ and various side hole radii.

Transmission spectra were measured using an optical spectrum analyzer and a tunable laser with a wavelength scan range of 1510–1640 nm. For simple cavities with three missing holes no resonance peak could be found most likely due to their low Q factors and resulting poor coupling efficiency. However, strong resonances were observed for the modified structures, as shown in Fig. 4(a). For these measurements, the polarization of the input light was adjusted to be TE relative to the PC slab. The maximum depth of the resonance was −2.6 dB achieved for the fundamental mode in cavity 1 with $a=560$ nm, $r=0.21a$, and $\Delta L=0.2a$ at the wavelength of 1550.7 nm. For cavity 2 where only a side hole shift of $\Delta L=0.15a$ was employed with a large lattice constant of 598 nm, two more resonance peaks were visible corresponding to higher order modes at shorter wavelengths with smaller amplitude and broader linewidth. Figure 4(b) shows the spectral dependence as a function of fiber to cavity separation. The strength of coupling and off-resonance loss increased with reducing separation, while the position of the resonance shifted towards longer wavelength due to a change in the effective index of the composite structure as the fiber approached. However, with sufficient air gap the taper does not significantly perturb the cavity modes, and the measured resonance linewidth $\delta\lambda$ obtained with a Lorentzian fit [see inset in Fig. 4(b)] was used to estimate the Q factors of the cavities using $Q=\delta\lambda/\lambda_o$ (where λ_o is the resonance wavelength).

The resulting Q factors and the corresponding numerical prediction are shown in Fig. 5. Figure 5(a) corresponds to the cavities with simple side hole shift. Due to our limited e-beam resolution, the maximum ΔL was set to be $0.2a$ for these samples. Figure 5(b) presents data for cavities with $\Delta L=0.2a$ with various hole radii. The two figures indicate that the measured Q values increase with increasing side hole shift and reducing radius following the trends predicted by the simulations. Compared to cavities with simple side hole shift, those where holes were both shifted and reduced in size gave higher Q which increased rapidly for radii below $0.24a$. The highest Q of $\approx 10\,000$ was obtained for a cavity with $r=0.19a$. The results were in agreement with the numerical predictions that showed that the combination of both a side hole shift and hole size reduction was required to obtain the highest Q values for a L3 cavity. Experiments on all-optical switching with these fabricated resonators are now under way. It is necessary to mention the astigmatism effect shown in Fig. 2. The shape of the holes was distorted, which was caused by misalignment of the e-beam writer or vertical tilt of the samples on the holder. Our latest experiments have shown that the distortion can be avoided by carefully aligning e-beam and samples. The effect of the elliptical hole on Q factor will be theoretically investigated soon by modifying our FDTD code.

The authors thank the Endeavor Australian Cheungkong award for financial support and the support of the Australian Research Council through its Federation Fellow and Centers of Excellence Programs. The key assistance of the laboratory members, especially Se-Heon Kim, Min-Kyo Seo, and Sun-Kyung Kim, from Nanolaser Laboratory, KAIST, is greatly appreciated. The authors thank Christian Grillet and Cameron Smith from the University of Sydney for data on one of the resonators.

[1] M. Notomi, A. Shinya, S. Mitsugi, G. Kira, E. Kuramochi, and T. Tanabe, Opt. Express **13**, 2678 (2005).
[2] T. Uesugi, B. Song, T. Asano, and S. Noda, Opt. Express **14**, 377 (2006).
[3] K. Ogusu, J. Yamasaki, S. Maeda, M. Kitao, and M. Minakata, Opt. Lett. **29**, 265 (2004).
[4] Y. Ruan, B. Luther-Davies, W. Li, A. Rode, V. Kolev, and S. Madden, Opt. Lett. **30**, 2605 (2005).
[5] V. Taeed, M. Shokooh-Saremi, L. Fu, D. Moss, M. Rochette, I. Littler, B. Eggleton, Y. Ruan, and B. Luther-Davies, Opt. Lett. **30**, 2900 (2005).
[6] D. Freeman, S. Madden, and B. Luther-Davies, Opt. Express **13**, 3079 (2005).
[7] C. Grillet, C. Smith, D. Freeman, S. Madden, B. Luther-Davie, E. Magi, M. J. Stee, and B. Eggleton, Opt. Express **14**, 1070 (2006).
[8] Y. Akahane, T. Asano, B. Song, and D. Noda, Opt. Express **13**, 1202 (2005).
[9] S. Cho and H. Jun, Nucl. Instrum. Methods Phys. Res. B **237**, 525 (2005).
[10] Y. Tanaka, T. Asano, Y. Akahane, B. Song, and S. Noda, Appl. Phys. Lett. **82**, 1661 (2003).
[11] I.-K. Hwang, G. Kim, and Y. Lee, IEEE J. Quantum Electron. **42**, 131 (2006).